ADVANCED MATERIALS
www.advmat.de

High-Contrast Photopatterning of Photoluminescence within Quantum Dot Films through Degradation of a Charge-Transfer Quencher

*Mario Tagliazucchi, Victor A. Amin, Severin T. Schneebeli, J. Fraser Stoddart, and Emily A. Weiss**

A method to create diffraction-limited high-contrast patterns of photoluminescence (PL) within films composed of CdSe@CdS@ZnS core-shell-shell colloidal quantum dots (QDs) and polyviologen (PV) is described. The photopatterning mechanism is photoinduced chemical degradation of the polyviologen, which in its pristine (pre-degraded) state quantitatively quenches the PL of the QDs by acting as a photo-oxidant. In recent years, QD-based light emission has emerged as a commercially viable display technology;[1] therefore, there is a need for simple and robust techniques to pattern emissive quantum-dot films.[2–7] There are two categories of patterning methods: i) those that pattern the QDs themselves, such as selective deposition of QDs using a template,[8,9] stamping,[2,4,5] photo-[3,7] and electron beam[10] polymerization, or photodissolution;[11] and ii) those in which the substrate is homogeneously coated with a thin film of QDs and then the PL is locally enhanced in selected areas by photoirradiation (either using a shadow mask[12,13] or a scanning laser beam).[14,15]

The second category, photoactivation techniques, is the simplest and most robust. Kotov, Liz-Marzán, and co-workers first demonstrated patterning by photobrightening of citrate-stabilized CdSe@CdS QDs through a shadow mask.[12] This method provides high contrast between irradiated and non-irradiated areas, but at the expense of large hypsochromic shifts of the PL peak (30–40 nm), and therefore does not allow independent control over emission intensity and wavelength. The Batteas group proposed photopatterning of CdSe QDs by photooxidation of the thiol-capping ligands.[14] This work demonstrated almost diffraction-limited resolution but suffered from non-ideal contrast (due to "background" fluorescence from non-irradiated regions) and also resulted in large hypsochromic shifts of the emission peak.

The major advantage of the method we demonstrate here is that we obtain high-contrast PL patterns while preserving the original emission properties of the QDs (PL energy and linewidth). Rather than enhancing the PL by photoetching the QD to remove surface-localized electron or hole traps inducing surface reconstruction, and/or detaching surface-bound ligands, we incorporate a sacrificial, degradable charge-transfer quencher into the QD film, deactivate it in selected regions by photoirradiation, and thereby return the QDs to their emissive state in irradiated regions. This strategy allows high-contrast patterns because the non-irradiated state is completely and robustly non-emissive.

We prepared layer-by-layer (LbL)-deposited films on glass comprising thioglycolate capped CdSe@CdS@ZnS (QDs) and either polyviologen or the non-redox-active polymer PDDA (poly(diallyldimethylammonium chloride)). We refer to these QD-polymer films, which each have 6.5 alternating bilayers of polymer and QDs (and are terminated by the polymer layer), as QD/PV and QD/PDDA, respectively. **Figure 1**A shows that these two films have similar absorption spectra; however, the PL spectrum of QD/PDDA exhibits a strong and narrow peak at 623 nm (Gaussian shape with full width at half maximum (FWHM) = 30 nm), while there is no detectable PL from QD/PV. The quantitative quenching of the QDs by PV can be understood in light of our previous studies, which demonstrated that ultrafast photoinduced electron transfer (PET) occurs from photoexcited CdSe QDs to viologen monomers in solution[16] and to PV in the solid state.[17] The time constant for PET in the CdSe@CdS@ZnS QD/PV film studied here is 26 ps (see Figure S3 in the Supporting Information). This time constant is much smaller than the reported values for the excited state lifetime for CdSe@CdS@ZnS QDs in the absence of PV (between 4 and 20 ns);[18–20] we can therefore conclude that PET quantitatively out-competes radiative recombination.

The PL of the QD/PV film is restored by photoirradiation of the film at energies greater than the bandgap of the QD (the photoactivation does not rely on direct photoexcitation of the PV). Figure 1B shows a series of PL spectra acquired during continuous photoirradiation of a QD/PV film with a 532-nm continuous-wave laser. Figure 1C shows the time evolution of the integrated PL peak area. Over 7 h of irradiation, the PL monotonically increases, but the spectral properties of the peak remain approximately constant: the PL peak position shifts from 619 nm to 615 nm and the peak FWHM is unchanged (FWHM = 28 nm). For reference, the PL-peak position and FWHM for the QDs in aqueous solution are 620 nm and 30 nm, respectively (Figure S2 in the Supporting Information). The PL peak area, position, and width of photoirradiated samples did not change after storage in the dark for four

Dr. M. Tagliazucchi, V. A. Amin, Dr. S. T. Schneebeli, Prof. J. F. Stoddart, Prof. E. A. Weiss
Department of Chemistry
Northwestern University
2145 Sheridan Rd., Evanston, IL 60208-3113, USA
E-mail: e-weiss@northwestern.edu

Prof. J. F. Stoddart
NanoCentury KAIST Institute and Graduate School of EEWS (WCU)
Korea Advanced Institute of Science and Technology (KAIST)
373-1 Guseong Dong, Yuseong Gu, Daejeon 305-701, Republic of Korea

DOI: 10.1002/adma.201201356

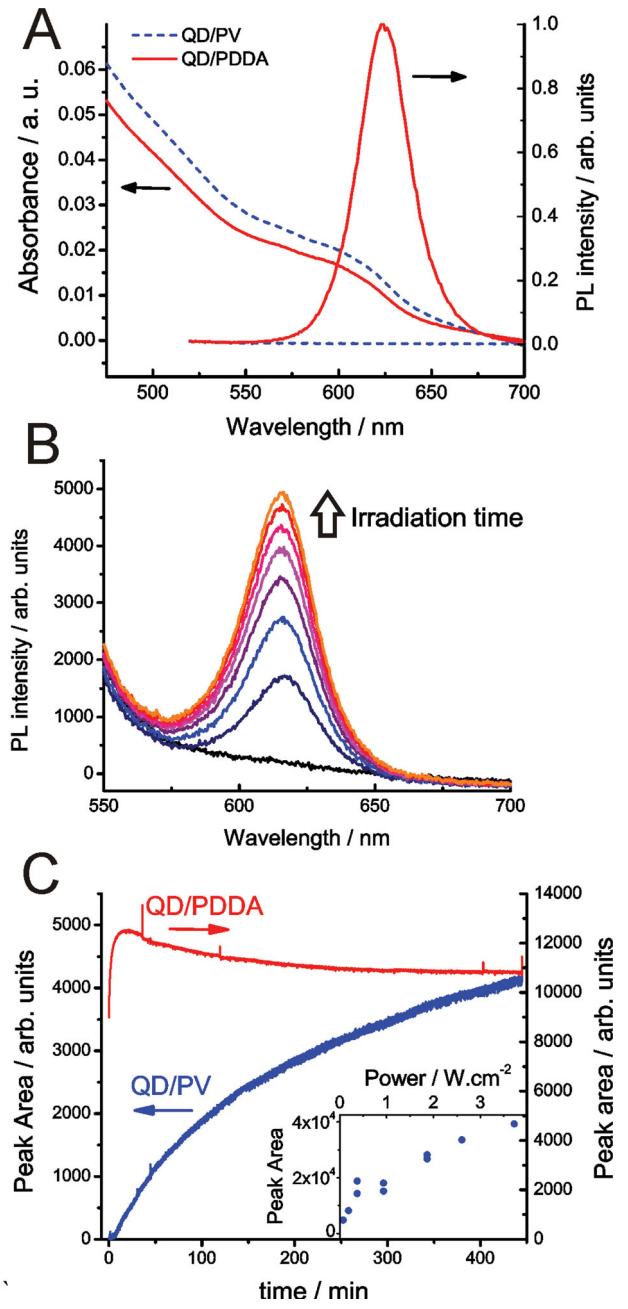

Figure 1. A) Ground-state absorbance (left axis) and photoluminesence (right axis) spectra for QD/PDDA (solid lines) and QD/PV (dashed lines) films (QD = CdSe@CdS@ZnS). B) Time evolution of the PL spectrum of a QD/PV film recorded during continuous illumination with a 532-nm continuous-wave laser (power: 3.6 W cm^{-2}). Curves (from bottom to top) correspond to irradiation times of 0, 60, 120, 180, 240, 300, 360, and 420 min. C) Peak area vs. irradiation time for QD/PV (left axis) and a QD/PDDA (right axis) films (using the same irradiation conditions as in (B)). Inset: peak area for QD/PV (measured under 1.8 W cm^{-2} illumination) after photoactivation for 120 min using different laser powers.

days (Figure S4 in the Supporting Information). This result indicates that PL restoration by degradation of PV is robust, while in many cases photobrightening methods produce PL enhancements that partially reverse on the timescale of hours.[15,21,22] The degradation of PV can be controlled both by the irradiation time and intensity. Figure 1C shows that, for a given irradiation time, the PL magnitude increases linearly with the irradiation power.

Figure 1C also shows the evolution of the PL-peak area for a QD/PDDA film (the "control film"). In this case, the PL increases ≈40% after 17 min and then slowly decreases; the peak position and width remained constant during the entire experiment. This evolution of PL, a combination of photobrightening followed by photodarkening, is commonly observed in photoirradiation experiments on QDs.[21,23] The magnitude of PL enhancement caused by photobrightening for QD/PDDA films (1.40 times) cannot account for the recovery of the PL in QD/PV films (at least 200 times, as we estimate from the noise of the PL spectrum of the unirradiated sample and the PL peak area after 7 h of irradiation). We can therefore conclude that photobrightening is not the dominant mechanism for restoring the PL in irradited QD/PV films.

The data in **Figure 2**A show that restoration of the PL of the film by photodegradation of PV relies on the presence of oxygen. Irradiation of a QD/PV film for 90 min under N_2(g) flow completely fails to restore the PL of the QDs; however, PL restoration begins immediately after replacement of N_2(g) by air. Attenuated total reflectance Fourier transform infrared (ATR-FTIR) spectroscopy experiments show that photoirradiation under air causes a decrease in the intensity of the characteristic IR bands of PV and the appearance of a new, as-yet unidentified, IR band (see Figure S5 in the Supporting Information); this result indicates chemical degradation of PV during irradiation. Previous studies revealed that the methyl viologen radical cation ($MV^{\bullet+}$), both in solution and solid state phases, reacts rapidly with oxygen to produce superoxide anion and methyl viologen (MV).[24,25] The as-formed superoxide anion then readily reacts with another $MV^{\bullet+}$ via radical–radical coupling.[26] In aprotic inert solvents, this reaction proceeds by degradation of one of the MV rings and formation of several decomposition products.[26] Based on our experimental results and these literature reports, we suggest that the decomposition of PV during photoirradiation involves the formation of $V^{+\bullet}$ upon PET from the photoexcited QDs to PV followed by its degradation mediated by oxygen. Figure 2B summarizes the proposed mechanism underlying PL restoration in the QD/PV films.

In **Figure 3** we demonstrate photopatterning of PL into QD/PV films. Figure 3A,B demonstrates large-area photopatterning using a shadow mask. In Figure 3C,D we show high-resolution photolithography by using a scanning laser beam of a confocal microscope to pattern single lines. In the experiment shown in Figure 3C, the films were patterned in contact with air (the objective and the QD/PV film were separated by a coverslip; we used immersion oil between the objective and the coverslip but not between the coverslip and the film). We fit the PL intensity profiles across the photopatterned lines with a sum of three Lorentzian functions to obtain an average FWHM of 778 nm ± 24 nm (left panel in Figure 3C). We improved the focus of the laser beam on the film by using immersion oil between the film and the coverslip; in these conditions, both the contrast and the resolution were

Adv. Mater. 2012,
DOI: 10.1002/adma.201201356

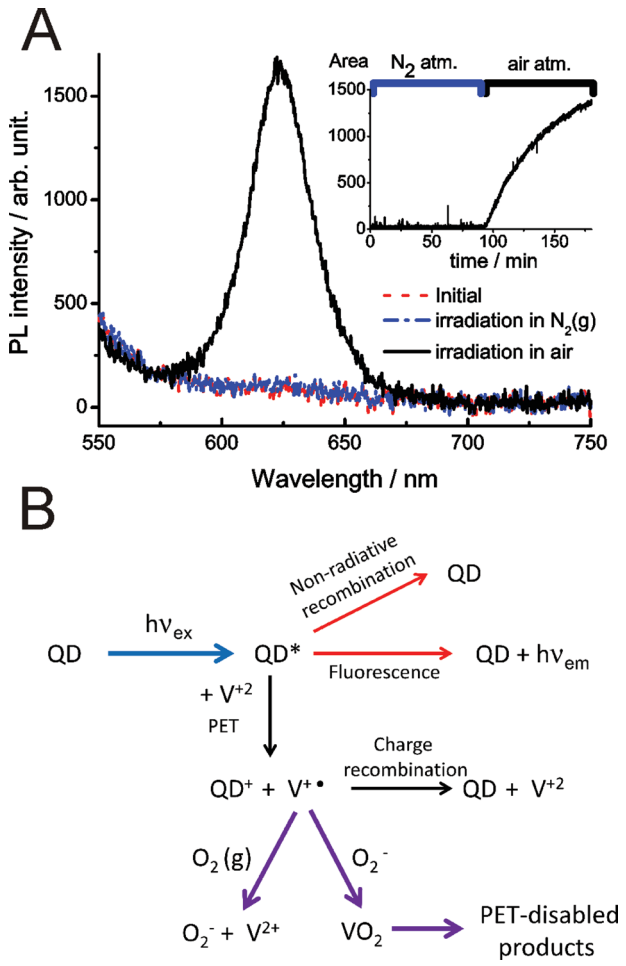

Figure 2. A) PL spectra of a QD/PV film before irradiation, after 90 min irradiation under dry N_2(g) atmosphere, and after additional 90 min irradiation in air (using the same irradiation conditions as in Figure 1B,C). Inset: peak area vs irradiation time. B) Proposed mechanism for PL enhancement in QD/PV films: in the presence of PV, photoinduced electron transfer (τ_{PET} = 26 ps) quantitatively out-competes radiative recombination (τ > 4–20 ns) as the decay mechanism for the excitonic state of CdSe@CdS@ZnS QDs. The reduced viologen radical cation $V^{+\bullet}$ reacts slowly with oxygen (probably via the formation of superoxide). Decomposition of viologen monomers within PV during prolonged or high-power photoexcitation eliminates the PET decay pathway and therefore restores the QD fluorescence.

enhanced (Figure 3D). The resolution of the line in Figure 3D is 576 nm ± 6 nm, which is consistent with twice the diffraction-limited resolution ($d \approx \lambda/2$ = 244 nm); this resolution is expected for this experiment since both the patterning and imaging processes are diffraction-limited.

In summary, we have demonstrated a new strategy to photopattern photoluminescence into QD thin films based on spatially selective photodegration of a polymeric charge-transfer quencher. Our strategy preserves the peak position and width of the original QD PL spectrum. Furthermore, our method allows photopatterning of films made of high-quality core/shell quantum dots, in contrast to previous methods that require lesser-quality QDs with trap-rich surfaces. It is interesting, for instance, to compare our experimental results for the photoirradiation of QD/PDDA (the control film) with the literature experiments for citrate-capped CdSe@CdS/PDDA films.[12] That work reported photoenhancement factors of >100 and very large hypsochromic shifts, while, for QD/PDDA, we observed a small intensity enhancement and no shift of the PL peak. The difference arises from the fact that our QDs are synthesized using an organometallic route and their light-emitting core is protected from photoetching by a ZnS shell, whereas the citrate-capped QDs are synthesized in water and have unpassivated, trap-rich surfaces (and broader PL peaks, FWHM >40 nm). Photo-oxidation by UV irradiation eliminates surface traps (and therefore brightens the sample) but also photoetches the QD surface to produce hypsochromic shifts.

The strategy presented in this paper to pattern the PL of QD films by incorporation of a degradable quencher can be further developed, for example, by engineering reversible photoswitchable quenchers[27] or using other (non-diffraction-limited) deactivation methods, such as scanning-probe electrochemical switching.[28] We believe that this category of PL-restoring techniques will provide a simple and robust method to prepare PL patterns for light-emitting devices.

Experimental Section

Materials: Poly(p-xylyl viologen)[17,29] and water soluble thioglycolate-capped CdSe@CdS@ZnS were synthesized following previously published protocols.[17,30,31] The Supporting Information describes the synthesis, purification, and characterization of these materials in detail. PDDA was acquired from Sigma-Aldrich and used without further purification.

Film Deposition: The QD/PV and QD/PDDA films were deposited on plasma-cleaned glass slides by LbL adsorption of QD, PV, and PDDA aqueous solutions. The LbL procedure is described in detail in the Supporting Information and in a previous publication.[17]

Steady-State PL of QD/PV and QD/PDDA Films: The PL spectra shown in Figure 1A were recorded using a Fluorolog-3 spectrofluorometer (Horiba JobinYvon Spex) equipped with a film-holder accessory using 500-nm light excitation. The photoactivation kinetics shown in Figure 1B,C and Figure 2A were acquired using the continuous-wave 532-nm laser beam from a laser pointer at an angle of 20° and focused to a 185-µm spot. The PL signal was collected and focused into a fiber optic coupled to a CCD detector (Jaz, Ocean Optics). For the experiments shown in Figure 2A, a home-built gas flow chamber connected to either N_2 or air was used (the gas was dried using a Drierite cartridge connected between the cell and the gas inlet). The power of the laser beam was measured using a photodiode detector after the sample and the peak area vs time plots in Figure 1C and Figure 2A (inset) were corrected to account for the fluctuation of the laser power (less than 10% during the whole experiment).

Confocal Microscopy and Scanning Laser Beam Patterning: Confocal images were acquired in a Zeiss LSM 510 Meta microscope using the 514-nm line of an Ar laser as the excitation source, a 560-nm-long-pass emission filter and a photodiode detector. Photopatterning using the scanning laser beam was performed using the photobleaching tools of the LMS 510 Software and the 488-nm line of the Ar excitation laser (30 mW). No photoactivation due to sample imaging was found (by zooming out after scanning a small region of the sample).

Supporting Information

Supporting Information is available from the Wiley Online Library or from the author.

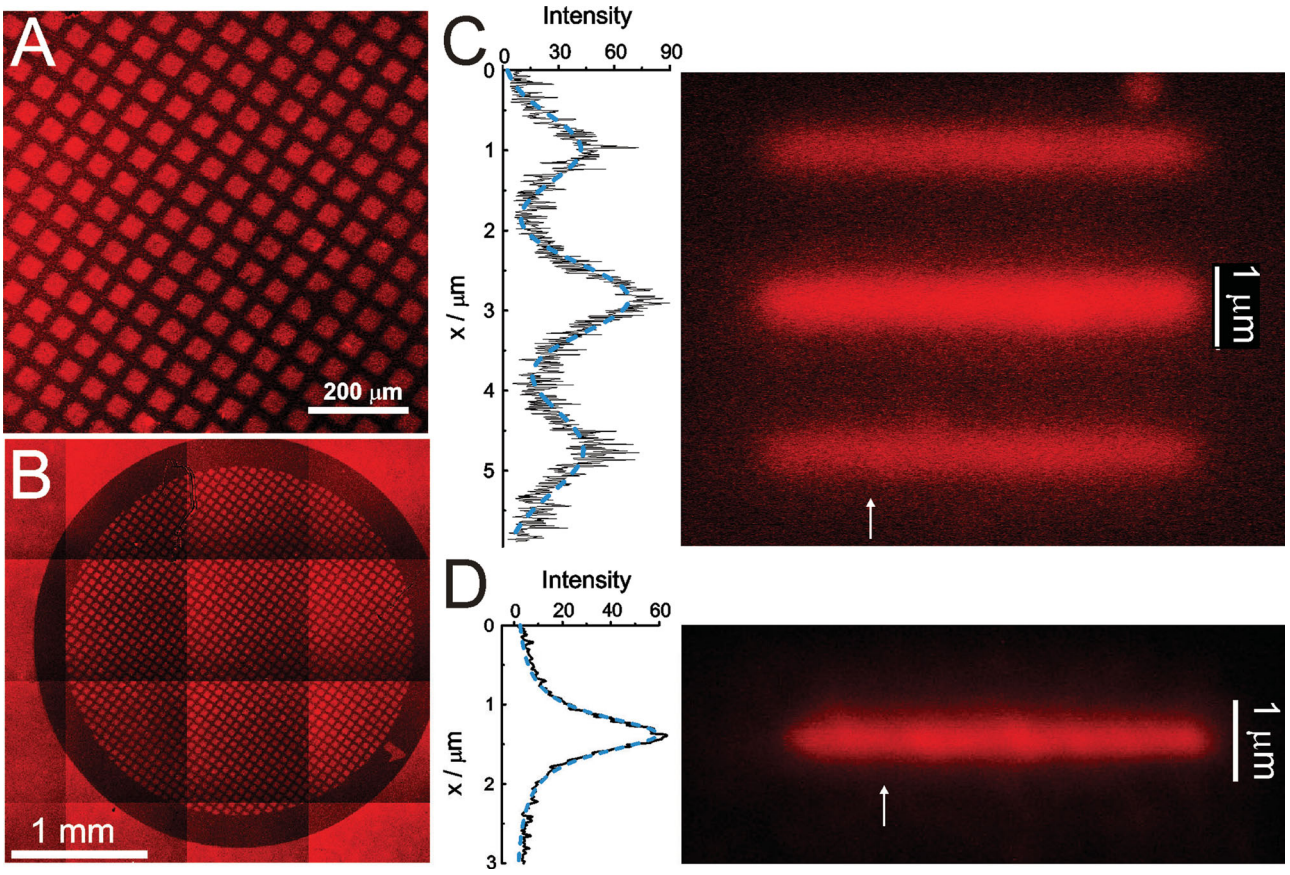

Figure 3. A) Confocal microscope image of a PL photopattern on a QD/PV film formed with a TEM-grid shadow mask and UV illumination (367 nm, 0.014 W cm^{-2} for 24 h) using a 20× objective. B) Same as panel A but using a 10× objective and tile reconstruction. C,D) Photolithography of a QD/PV film using the scanning laser beam of a confocal microscope (488 nm, 100× objective, NA = 1.45). The film was patterned in contact with air (C) or immersion oil (D), see the main text for a description of the experimental set-up. Irradiation times of 6, 12, and 6 min were used for the lines in (C) (from up to bottom) and 3 min for the line in (D). The plot on the left shows the PL intensity profile along the line marked by the white arrow. The dashed curve is the best fit to the profiles using Lorentzian functions with FWHM of 654 nm ± 24 nm, 790 nm ± 18 nm, 890 nm ± 29 nm for the lines in (C) (from top to bottom) and 576 nm ± 6 nm for the line in (D).

Acknowledgements

This material is based upon work supported as part of the NERC (Non-Equilibrium Research Center), an Energy Frontier Research Center funded by the U.S. Department of Energy, Office of Science, Office of Basic Energy Sciences under Award Number DE-SC0000989. S.T.S. thanks the International Institute for Nanotechnology at Northwestern University for a postdoctoral fellowship. J.F.S. and S.T.S. were supported by the WCU Program (NRF R-31-2008-000-10055-0) funded by the Ministry of Education, Science and Technology, Korea. The authors thank Paul T. Brannon and Dr. Nathan A. Mathew for their assistance with the confocal microscope and the steady-state fluorescence measurement, respectively. This work used instruments located in the NUANCE Center facilities, which are supported by the NSF-MRSEC, NSF-NSEC, and the Keck Foundation. Confocal microscopy was performed in the Biological Imaging Facility (BIF) at Northwestern University.

Received: April 3, 2012
Revised: May 13, 2012
Published online:

[1] J. A. Smyder, T. D. Krauss, *Mater. Today* **2011**, *14*, 382.
[2] T.-H. Kim, K.-S. Cho, E. K. Lee, S. J. Lee, J. Chae, J. W. Kim, D. H. Kim, J.-Y. Kwon, G. Amaratunga, S. Y. Lee, B. L. Choi, Y. Kuk, J. M. Kim, K. Kim, *Nat. Photonics* **2011**, *5*, 176.
[3] J.-J. Park, P. Prabhakaran, K. K. Jang, Y. Lee, J. Lee, K. Lee, J. Hur, J.-M. Kim, N. Cho, Y. Son, D.-Y. Yang, K.-S. Lee, *Nano Lett.* **2010**, *10*, 2310.
[4] A. Gopal, K. Hoshino, X. Zhang, *Appl. Phys. Lett.* **2010**, *96*.
[5] L. Kim, P. O. Anikeeva, S. A. Coe-Sullivan, J. S. Steckel, M. G. Bawendi, V. Bulovic, *Nano Lett.* **2008**, *8*, 4513.
[6] Y. T. Chan, P. T. Snee, J. M. Caruge, B. K. Yen, G. P. Nair, D. G. Nocera, M. G. Bawendi, *J. Am. Chem. Soc.* **2006**, *128*, 3146.
[7] S. Jun, E. J. Jang, J. Park, J. Kim, *Langmuir* **2006**, *22*, 2407.
[8] S. Jaffar, K. T. Nam, A. Khademhosseini, J. Xing, R. S. Langer, A. M. Belcher, *Nano Lett.* **2004**, *4*, 1421.
[9] Y. Babayan, J. E. Barton, E. C. Greyson, T. W. Odom, *Adv. Mater.* **2004**, *16*, 1341.
[10] V. Nandwana, C. Subramani, Y.-C. Yeh, B. Yang, S. Dickert, M. D. Barnes, M. T. Tuominen, V. M. Rotello, *J. Mater. Chem.* **2011**, *21*, 16859.

[11] Y. Park, M. J. Felipe, R. C. Advincula, *ACS Appl. Mater. Interfaces* **2011**, *3*, 4363.
[12] Y. Wang, Z. Y. Tang, M. A. Correa-Duarte, L. M. Liz-Marzan, N. A. Kotov, *J. Am. Chem. Soc.* **2003**, *125*, 2830.
[13] X. Chen, A. L. Rogach, D. V. Talapin, H. Fuchs, L. Chi, *J. Am. Chem. Soc.* **2006**, *128*, 9592.
[14] J. Chen, Y.-H. Chan, T. Yang, S. E. Wark, D. H. Son, J. D. Batteas, *J. Am. Chem. Soc.* **2009**, *131*, 18204.
[15] T. Uematsu, J. Kimura, Y. Yamaguchi, *Nanotechnology* **2004**, *15*, 822.
[16] A. J. Morris-Cohen, M. T. Frederick, L. C. Cass, E. A. Weiss, *J. Am. Chem. Soc.* **2011**, *133*, 10146.
[17] M. Tagliazucchi, D. B. Tice, C. M. Sweeney, A. J. Morris-Cohen, E. A. Weiss, *ACS Nano* **2011**, *5*, 9907.
[18] M. Jones, S. S. Lo, G. D. Scholes, *Proc. Natl. Acad. Sci. USA* **2009**, *106*, 3011.
[19] Y. Fu, H. Agren, J. M. Kowalewski, H. Brismar, J. Wu, Y. Yue, N. Dai, L. Thylen, *EPL* **2009**, *86*.
[20] S. J. Lim, B. Chon, T. Joo, S. K. Shin, *J. Phys. Chem. C* **2008**, *112*, 1744.
[21] S. R. Cordero, P. J. Carson, R. A. Estabrook, G. F. Strouse, S. K. Buratto, *J. Phys. Chem. B* **2000**, *104*, 12137.
[22] D. B. Tice, M. T. Frederick, R. P. H. Chang, E. A. Weiss, *J. Phys. Chem. C* **2011**, *115*, 3654.
[23] H. Asami, Y. Abe, T. Ohtsu, I. Kamiya, M. Hara, *J. Phys. Chem. B* **2003**, *107*, 12566.
[24] K. B. Yoon, J. K. Kochi, *J. Am. Chem. Soc.* **1988**, *110*, 6586.
[25] J. A. Farrington, M. Ebert, E. J. Land, K. Fletcher, *Biochim. Biophys. Acta* **1973**, *314*, 372.
[26] E. J. Nanni, C. T. Angelis, J. Dickson, D. T. Sawyer, *J. Am. Chem. Soc.* **1981**, *103*, 4268.
[27] S. A. Diaz, G. O. Menendez, M. H. Etchehon, L. Giordano, T. M. Jovin, E. A. Jares-Erijman, *ACS Nano* **2011**, *5*, 2795.
[28] A. B. Braunschweig, A. J. Senesi, C. A. Mirkin, *J. Am. Chem. Soc.* **2009**, *131*, 922.
[29] A. Factor, G. E. Heinsohn, *J. Polym. Sci. Part B: Polym. Lett.* **1971**, *9*, 289.
[30] J. J. Li, Y. A. Wang, W. Z. Guo, J. C. Keay, T. D. Mishima, M. B. Johnson, X. G. Peng, *J. Am. Chem. Soc.* **2003**, *125*, 12567.
[31] J. Aldana, Y. A. Wang, X. Peng, *J. Am. Chem. Soc.* **2001**, *123*, 8844.